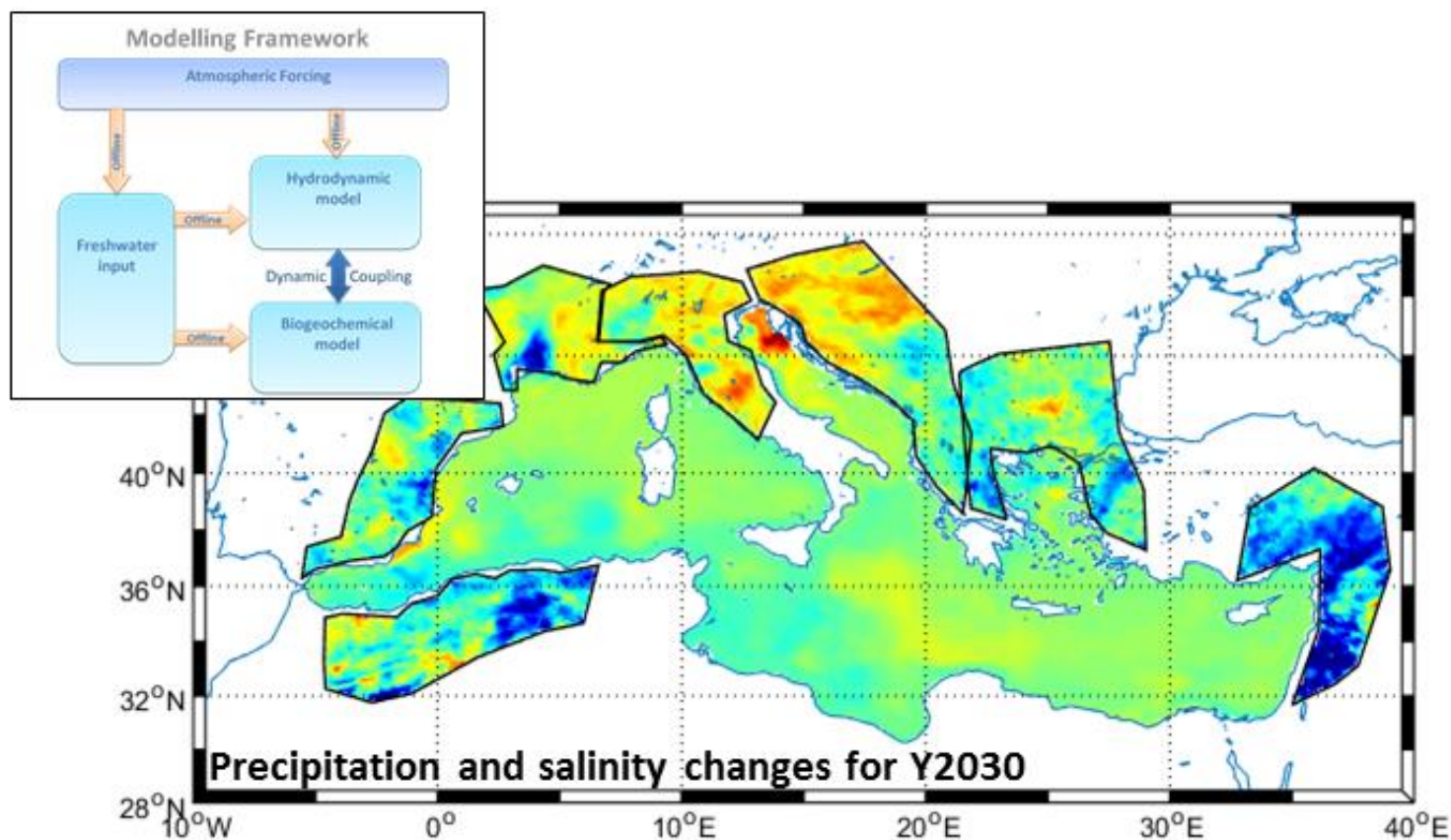


JRC TECHNICAL REPORTS

Multi-year simulations of future socio-economic and climate scenarios in the Mediterranean Sea

Macias, Diego; Stips, Adolf; Garcia-Goriz, Elisa

2016



This publication is a Technical report by the Joint Research Centre (JRC), the European Commission's science and knowledge service. It aims to provide evidence-based scientific support to the European policy-making process. The scientific output expressed does not imply a policy position of the European Commission. Neither the European Commission nor any person acting on behalf of the Commission is responsible for the use which might be made of this publication.

Contact information

Name: Diego M. Macias Moy
Address: Joint Research Centre. Directorate D. Ispra, Italy
E-mail: diego.macias-moy@jrc.ec.europa.eu
Tel.: +39 0332 789636

JRC Science Hub

<https://ec.europa.eu/jrc>

JRC103933

EUR 28384 EN

PDF 978-92-79-64819-9 ISSN 1831-9424 doi:10.2788/386552

Luxembourg: Publications Office of the European Union, 2016

© European Union, 2016

Reproduction is authorised provided the source is acknowledged.

How to cite: Macias Moy D; Stips A; Garcia Gorriz E.; *Multi-year simulations of future socio-economic and climate scenarios in the Mediterranean Sea*; Luxembourg (Luxembourg): Publications Office of the European Union; 2016; EUR 28384; doi:10.2788/386552

All images © European Union 2016

Table of contents

Abstract	1
1 Introduction	2
2 Material and Methods	3
2.1 Ocean Model.....	3
2.2 Regional Climate Models	4
2.3 Rivers' Scenarios.....	5
2.3.1 Freshwater flow modifications.....	5
2.3.2 Nutrients modifications.....	8
2.3.3 Model runs with modified rivers' conditions	10
3 Results	11
3.1 Evolution of the basin in the 'baseline' simulations	11
3.2 Evolution of the hydrodynamic and biogeochemical conditions in the rivers' scenarios runs.....	13
4 Conclusion	19
References	21
List of abbreviations and definitions.....	23
List of figures.....	24
List of tables.....	25

Abstract

The Modelling Framework for European regional seas developed at unit D02 of the JRC is applied to explore plausible consequences for the Mediterranean Sea marine ecosystems of a set of climate and socio-economic scenarios for the 2030 horizon. The main objective of this work is to test the capability of the Modelling Framework to perform scenario forecasts. Therefore an ensemble of two different regional climate models under two selected emissions scenarios are combined with two socio-economic pathways to force a single hydrodynamic-biogeochemical ocean model. Socio-economic alternatives are reflected in the modelling system through changes in the river water quality (nutrient levels) that are flowing into the ocean basin. A step-wise approach allows to compare the different scenarios (combination of climate and socio-economic changes) and to quantify the induced changes in the marine ecosystem status. The model performance and the achieved results are strongly influenced by the reliability of the applied hydro-meteorological forcings. The applicability of the Modelling Framework to this type of scenario investigations could be successfully demonstrated.

1 Introduction

The Mediterranean Sea is one of the main EU regional seas and has been described as a hot-spot for climate change (Giorgi, 2006) because of a number of reasons. Firstly, it is located in a temperate region which is expected to become warmer and drier in the nearby future (IPCC, 2013). Secondly it is a semi-enclosed basin being, thereby, strongly influenced by continental conditions. Thirdly, it hosts a very large human population that exerts a considerable influence on the marine ecosystems' conditions (e.g., Macias et al., 2014a).

Thus, climatic and anthropogenic forcings would combine in the future in uncertain ways and will potentially create a wide range of pressures on the Mediterranean Sea ecosystems. EU-wide political measures concerning, for example, waste-water treatments or manure and agricultural management could also change the chemical quality of the freshwater flow into the basin with uncertain consequences for its ecosystem status.

Henceforth, one of the only ways to try to assess expected future consequences is through scenario generation using a set of numerical interconnected models (Najjar et al., 2000). Three elements should, at least, be included in the scenario generation process, the atmosphere, the ocean and the socio-economic activity. With such interconnected models, attribution exercises could be performed by isolating sources of variability and assessing potential changes on the variables of interest by the individual forcing factors (e.g., atmospheric conditions, river discharges or human activities).

For this specific aim, the Joint Research Centre (JRC) of the EU Commission is developing the Modelling Framework (MF) for EU regional seas (Garcia-Gorriz et al., 2016; Stips et al., 2015) which include the main elements of a Regional Earth System Model, *i.e.*, the atmosphere, the hydrological basin and the oceans. Several implementations of the MF do exist within the JRC, but here we use an ocean model already proven to provide a reasonable representation of past and present hydrodynamic and biogeochemical conditions of the Mediterranean basin (Macias et al., 2013, 2014a, 2014b) to explore a set of future scenarios for the basin.

This ocean model is forced at the surface with atmospheric variables provided by a regional circulation model (RCM) forced at the boundaries with different global climate models (GCMs) included in the Coupled Model Intercomparison Project Phase 5 CMIP5 exercise. Different emission scenarios for each GCM (rcp4.5 and rcp8.5) are considered. This MF setup has been already used to perform continuous forecasts from 2013 to 2100 assuming non-changing rivers' conditions in Macias et al. (2015) in order to evaluate the effect on the marine ecosystem of a changing climate. In this occasion scenarios simulations for year 2030 are made assuming both freshwater flow changes due to changes in precipitation values and in freshwater quality (mainly nutrient concentrations) according to different socioeconomic pathways. These new sets of simulations are compared with the ones performed with constant rivers (*i.e.*, those from Macias et al., 2015) in order to quantify and isolate the effects of changing freshwater conditions.

The main aim of this report is not to provide plausible future scenarios for the Mediterranean basin for the 2030 horizon but, rather, to evaluate the performance, potential and shortcomings of the MF to perform such forecasting exercises. More specific, policy-oriented scenarios should be tested in the near future with the assistance of policy DGs.

2 Material and Methods

We have used a reduced version of the Modelling Framework (MF) for EU regional marine seas (Fig. 1) applied to the Mediterranean Sea. The ocean model is composed of two interconnected (on-line coupled) components, the GETM hydrodynamic model (Stips et al., 2004) and MedERGOM biogeochemical model (Macias et al., 2014b) (Fig. 1 and section 2.1 below). As atmospheric forcing for this ocean model we used the climatic simulations provided by the Regional Climate Model (RCM) COSMOS-CLM (Fig. 1 and section 2.2 below). The lateral boundary conditions for freshwater flow and nutrient levels (Fig. 1) are computed following the rationale exposed in section 2.3 below).

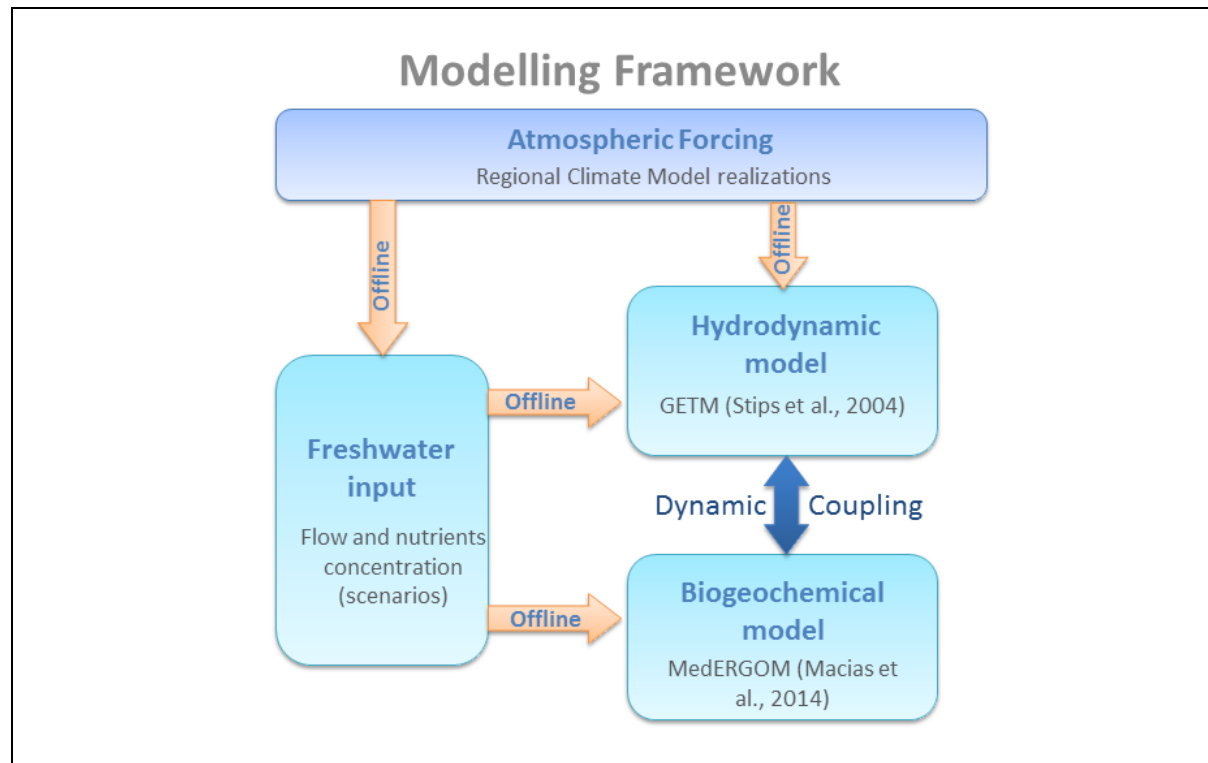


Figure 1. Modelling Framework (MF) scheme as used in the present report.

2.1 Ocean Model

The 3-D General Estuarine Transport Model (GETM) was used to simulate the hydrodynamics in the Mediterranean Sea. GETM solves the three-dimensional hydrostatic equations of motion applying the Boussinesq approximation and the eddy viscosity assumption (Burchard and Bolding, 2002). A detailed description of the GETM equations could be found in Stips et al. (2004) and at <http://www.getm.eu>.

The configuration of the Mediterranean Sea (Fig. 2) has a horizontal resolution of 5' x 5' and includes 25 vertical sigma-layers. A third-order Total Variation Diminishing (TVD) numerical scheme is used as recommended by Burchard et al. (2006). ETOPO1 (<http://www.ngdc.noaa.gov/mgg/global/>) was used to build the bathymetric grid by averaging depth levels to the corresponding horizontal resolution of the model grid. The salinity and temperature climatologies used as initial conditions at the start of the model integration were obtained from the Mediterranean Data Archeology and Rescue-MEDAR/MEDATLAS database (<http://www.ifremer.fr/medar/>) while biogeochemical initial and boundary conditions were computed from the World Ocean Atlas database (www.nodc.noaa.gov/OC5/indprod.html). The model was initially run during the period 1996 – 2012 to reduce the effect of the imposed initial conditions. Model results for December 2012 were used to initialize the scenario runs (2013 – 2035) described below.

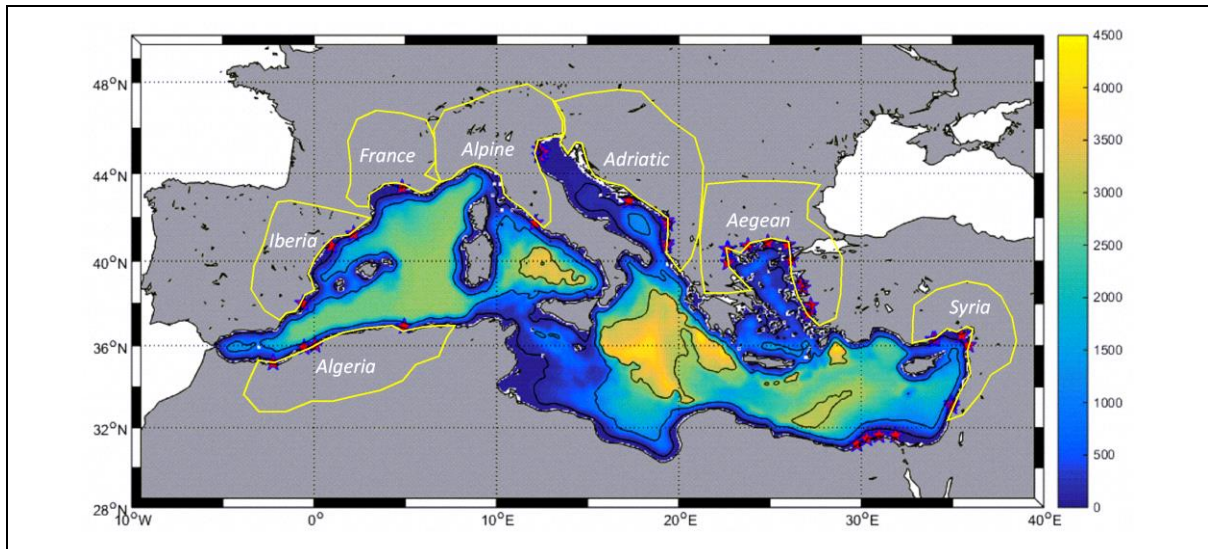


Figure 2. Model domain, bathymetry (background scale), included rivers (red stars) and polygons (yellow lines) defining the different regions considered for rivers' basins.

Boundary conditions at the western entrance of the Strait of Gibraltar were also computed from the same MEDAR/MEDATLAS dataset imposing monthly climatological vertically explicit values of salinity. Sea surface temperature at the western entrance of the Strait was extracted from the nearest node of the driven GCM for each simulation (see below) while the rest of the water column temperature was not changed. No explicit boundary condition for horizontal currents was imposed at the open boundary. With this boundary configuration the circulation through the Strait is established by the internally-adjusted baroclinic balance provoked mainly by the deep-water formation within the basin (Macias et al., 2016a).

GETM is coupled online to the MedERGOM biogeochemical model (Macias et al., 2014a and 2014b) by using the Framework for Aquatic Biogeochemical Models (FABM, <https://sourceforge.net/projects/fabm/>)(Brueggeman and Bolding, 2014). MedERGOM is a modified version of the ERGOM model (Neumann, 2000) specifically adapted to represent the conditions of the pelagic ecosystem of the Mediterranean Sea. It has proven useful to describe present (Macias et al., 2014a), past (Macias et al., 2014b) and future (Macias et al., 2015) biogeochemical conditions in this semi-enclosed basin.

2.2 Regional Climate Models

The ocean model described above is forced at the surface (see scheme in Fig. 1) with the outputs from the COSMO-CLM RCM (<http://www.clm-community.eu/>), in the framework of the EURO-CORDEX initiative (<http://www.euro-cordex.net/>). The RCM is forced by two GCMs, namely EC-Earth and MPI-ESM-MR included in the CMIP5 (Table 1). The RCM spatial resolution is 0.11°. For each GCM two emission scenarios as defined by IPCC are considered; rcp4.5 and rcp8.5 (Meinshausen et al., 2011).

Modelling group	Driving model name	Emission scenarios
ECEARTH consortium	EC-EARTH	rcp 4.5 / rcp 8.5
Max-Planck-Institut für Meteorologie (Max Planck Institute for Meteorology)	MPI-ESM-MR	rcp 4.5 / rcp 8.5

Table 1. Institutes/modelling groups providing the atmospheric model data used in the present contribution.

As a necessary previous step to the Mediterranean runs and as concluded in Macias et al. (2016b), we have carried out a bias-correction of the most relevant atmospheric variables: air temperature, cloud cover and wind intensity. As shown in Macias et al. (2016b), the atmospheric variables provided by the RCM realizations induce a severe underestimation of simulated sea surface temperature (SST) for the present-day. The basic principle of the bias-correction technique consists in finding a transfer function that allows matching the cumulative distribution functions (CDFs) of modeled and observed data (Dosio and Paruolo, 2011; Dosio et al., 2011; Dosio, 2016). In our study, spatially-averaged values of the observed and model atmospheric variables over the entire Mediterranean Sea basin were used, so no spatially explicit correction was applied. A detailed description of the bias-correction technique and evaluation over the present climate is found at Macias et al., (2016b).

2.3 Rivers' Scenarios

2.3.1 Freshwater flow modifications

The present configuration of the ocean model includes 37 rivers discharging along the Mediterranean coast (red stars in Fig. 2). The present-day values for river discharges were derived from the Global River Data Center (GRDC, Germany) database while nutrient loads (nitrate and phosphate) of freshwater runoff were obtained from Ludwig et al. (2009). We, then, compute the seasonal climatological values of water flow and nutrient concentration for each river for the period 1985 – 2000. Using this climatological rivers conditions, four full-time scenario simulations covering the period 2013 – 2035 were performed using the four RCM realizations described above (MPI & EcEarth under RCPs 4.5 and 8.5). These continuous (2013 - 2035) model runs provide the 'baseline' scenario conditions for the comparisons below, as they only consider the impacts of atmospheric forcing changes (e.g., Macias et al., 2015).

To estimate potential changes in freshwater flow in the different climate scenarios, a proxy was created by evaluating the relative change on precipitation over the different rivers' catchments for year 2030 in a similar way as done by Somot et al. (2006). First of all, we defined the regions containing river catchments following the definition of the Water Information System for Europe (WISE) river basin districts (<http://www.eea.europa.eu/data-and-maps/data/wise-river-basin-districts-rbds-1>) but grouping together sets of rivers sharing a common catchment area. This way, 8 different 'provinces' have been defined as indicated in Table 2 and also shown in Fig. 2. Unfortunately, the catchment area for the Nile is not included within the EURO-CORDEX domain, so for this river no scenario on water flow changes could be derived from the used RCM. However, as indicated in previous works (Somot et al., 2006), no big alterations of the freshwater flow are to be expected for the Nile.

Region	Rivers included in the GETM domain
<i>Iberia</i>	Llobregat Ebro Jucar
<i>France</i>	Rhone
<i>Alpine</i>	Adige Po Tiber
<i>Adriatic</i>	Neretva Bojana Mati Vijosa
<i>Aegean</i>	Meric Nestos Gediz Bakircay Buyuk Kucuk Strimon Axios Pinios
<i>Syria</i>	Yarmuk Ceyhan Asi Goeksu Nahraz
<i>Nile</i>	Nile
<i>Algeria</i>	Meulouya Bouselam Chelif Tafna

Table 2. Basin names and included rivers.

For the rest of the basins/ rivers it is possible to compute relative changes of precipitation (P) between the first three years of the forecasting period (2014 – 2016) and years 2029 – 2031 for each combination of GCM/rcp. The annual average changes in P values for each model/emission scenario are shown in Table 3 (baseline river discharge = 290 km³/y). For the MPI model under the two evaluated emission scenarios, freshwater flow will decrease in year 2030 between 0.35% (rcp8.5) and 0.2 % (rcp4.5). For Ec-Earth realizations, the total freshwater flow will increase by about 1.1% (rcp4.5) and 0.4% (rcp8.5).

Model / emission scenario	Freshwater flow change (% of baseline values)
MPI/rcp4.5	-14.8 km ³ /y (-0.2%)
MPI/rcp8.5	-24.9 km ³ /y (-0.35%)
EcEarth/rcp4.5	+72.3 km ³ /y (+1.1%)
EcEarth/rcp8.5	+27.8 km ³ /y (+0.39%)

Table 3. Computed annual changes in freshwater flow for the different model/rcp combinations.

In order to consider also the seasonality of the potential changes, the climatological P cycles for the first 3 years of the RCM realization (2014 – 2016) are compared to the climatological P cycles during the later period (2029 – 2031). The percentage of change for each river's basins are shown in Fig. 3 for the different model/emission scenario combination.

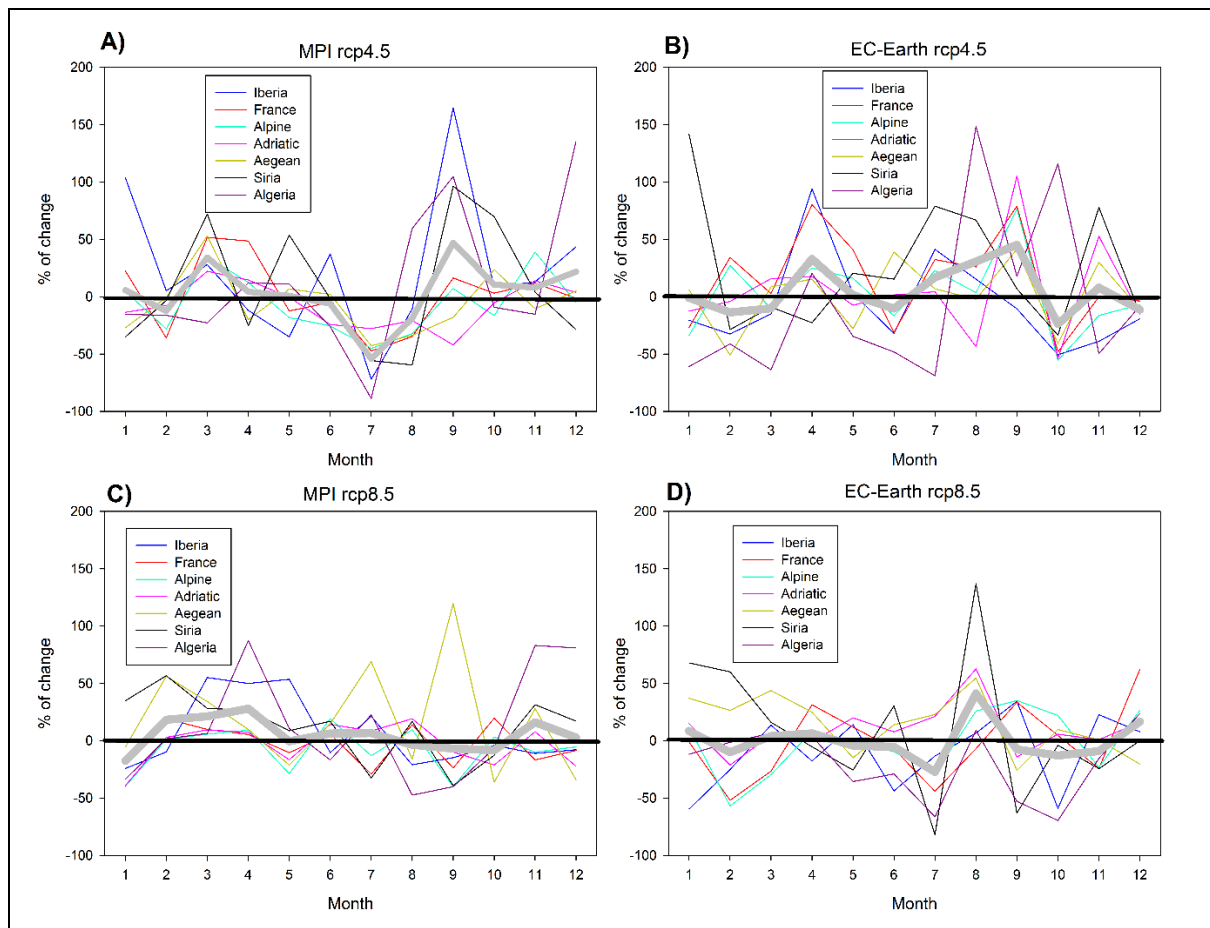


Figure 3. Relative change on P for each catchment area for MPI rcp4.5 scenario (A), EC-Earth rcp4.5 scenario (B), MPI rcp8.5 scenario (C) and EC-Earth rcp8.5 scenario (D). The 0% change level is indicated with a black line and the mean monthly change with a bold grey line.

In Fig. 3A, corresponding to the MPI-rcp4.5 realization, it could be seen that in most catchments future P decrease will occur mainly during summer while in winter/spring and during fall they tend to remain close to actual values or could slightly increase. For the same model (MPI) under rpc8.5 (Fig. 3B) the larger decrease is concentrated in the end of the summer/beginning of fall with winter month typically showing positive anomalies. The maps of mean anomalies for this GCM (Figs. 4A and 4C) show a generalized reduction of P in north-central river basin districts with the western and eastern districts showing positive anomalies. Both, maximum and minimum anomalies are larger in rpc8.5 (Fig. 4C) than in rpc4.5 (Fig. 4A).

No clear seasonal pattern could be identified on the EC-Earth forced scenarios (Figs. 3B and 3C) as they show a much larger inter-catchment variability. The spatial distribution of the P anomalies for this model (Figs. 4B and 4D) show a different pattern than MPI, with the northern-central part of the Mediterranean becoming wetter in the future, especially under rpc8.5.

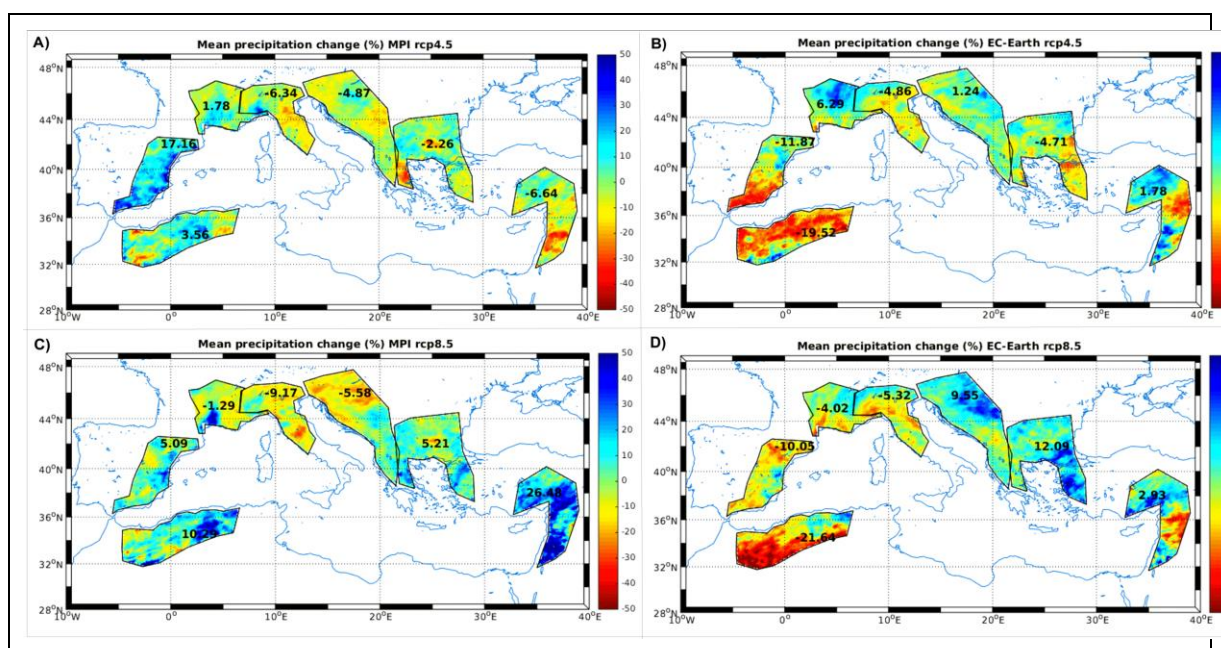


Figure 4. Mean P change (%) for each river basin district and model/RCP combination.

The monthly coefficients of relative changes for each model/emission scenario shown in Fig. 3 are used to generate new water flows in each river for the future conditions by multiplying these coefficients by the present-day freshwater flow values.

2.3.2 Nutrients modifications

Changes in nutrient loads for Mediterranean rivers are much more difficult to assess than flow changes as they are heavily dependent on socio-economic factors. For our ocean model we are mainly concerned on macronutrients and, more specifically, on nitrate and phosphate. Although information of potential changes is very scarce, there is a very relevant publication that could be used to our purposes, the paper by Ludwig et al. (2010). In there, potential changes on nitrogen and phosphate loads for different Mediterranean and Black Sea rivers are defined for years 2030 and 2050 under four different socio-economic scenarios used in the 'Millennium Ecosystem Assessment' exercise (Carpenter et al., 2006) (Table 4).

Scenario name	Description
TG: <i>Technogarden</i>	TG depicts a globally connected world relying strongly on technology and on highly managed and often engineered ecosystems to deliver needed goods and services. Overall, eco-efficiency improves, but it is shadowed by the risks inherent in large - scale human-made solutions.
OS: <i>Order from Strength</i>	OS represents a regionalized and fragmented world concerned with security and protection, emphasizing primarily regional markets and paying little attention to common goods, and with an individualistic attitude toward ecosystem management.
AM: <i>Adaptive Mosaic</i>	AM depicts a fragmented world resulting from discredited global institutions. It sees the rise of local ecosystem management strategies and the strengthening of local institutions. Investments in human and social capital are geared toward improving knowledge about ecosystem functioning and management
GO: <i>Global Orchestration</i>	GO depicts a worldwide connected society in which global markets are well developed. Supranational institutions are well placed to deal with global environmental problems. However, their reactive approach to ecosystem management makes them vulnerable to surprises arising from delayed action or unexpected regional changes.

Table 4. Socio-economic scenarios considered in the Millennium Ecosystem Assessment

Ludwig et al. (2010) provide changes on total nutrient loads ($kt\ y^{-1}$) for different rivers for each scenario shown above and for the years 2030 and 2050. Henceforth those changes (provided in table 4 of their paper) incorporate both changes due to concentration alteration and because of freshwater flow changes. To calculate the nutrients concentration changes alone we need to correct the reported load data with respect to the changes in water flows (provided in table 2 of their paper).

The relative changes of nutrient concentrations for each catchment under each specific scenario are, thus, compiled in table 5. As it would be very time-consuming in computer-time and difficult to run and analyse all four socioeconomic scenarios under the four climate models realizations ($4 \times 4 = 16$ runs + 4 runs with constant nutrients + 4 runs with constant water and nutrients = 24 runs), we selected the best (largest nutrient load reduction) and worst (largest nutrient load increase) socioeconomic scenarios. From our computations, the best case scenario corresponds to the TG (green boxes in table 5) and the worst case scenario to GO (red boxes in table 5).

	TG		AM		GO		OS	
Nutrient	Nitrate	Phosphate	Nitrate	Phosphate	Nitrate	Phosphate	Nitrate	Phosphate
Iberia	-33.3%	+50%	-37.5%	+50%	-25%	+50%	-33.3%	+50.0%
France	-12.2%	-	-17.8%	-	+7.8%	-	+42.2%	+16.0%
Alpine	-28.4%	-	-27.7%	-	-6.1%	-	-1.6%	-
Adriatic	-26.4%	-7.2%	-21.2%	-7.1%	+4.5%	-	-4.8%	-
Aegean	-21.3%	+8.3%	-21.7%	+8.3%	+0.5%	+8.3%	-10.8%	+8.3%
Syria	+17.9%	+25%	+20.5%	+25%	+28.2%	+25%	+30.7%	+25%
Argelia	-57.9%	+20%	-57.9%	+20%	-42.1%	+20%	-42.1%	+16.6%

Table 5. Relative change of nutrient concentration in freshwater for the different catchments and under the different scenarios.

2.3.3 Model runs with modified rivers' conditions

We used the initial conditions corresponding to January 2025 in the baseline simulations to start a 10 year simulation (2025 -2034) with the modified freshwater conditions for each model/scenario combination. The mean conditions from 2031 – 2034 were compared with the same years in the simulation with the climatologic rivers (*i.e.*, the baseline simulation). See a resume of the performed simulations in table 6.

Simulation	Atmospheric forcings	Rivers conditions	Initial conditions	Simulated period
Baseline	MPI & Ec-Earth (rcp 4.5 & 8.5)	Climatologic flow and nutrients (1985- 2000)	Results from model spin-off run for Jan 2013	2013 – 2035
Altered rivers	MPI & Ec-Earth (rcp 4.5 & 8.5)	Modified as described in section 2.3	Results from the corresponding baseline simulation for Jan 2025	2025 - 2035

Table 6. Description of the different model runs.

3 Results

3.1 Evolution of the basin in the 'baseline' simulations

Before discussing the effects of the riverine conditions and to better frame the comparison, we will describe briefly the transient simulations from 2013 to 2035 maintaining unaltered river conditions (i.e., the baseline simulations).

The mean annual values of surface properties (sea surface temperature (SST), sea surface salinity (SSS) and primary production rate (PPR)) are shown in Fig. 5 for all four model realizations. Regarding SST (Fig. 5A) no evident trend could be observed for any GCM/rcp combination but mostly interannual variability. This is not unexpected because as shown by Macias et al. (2015) the SST trajectories of the different scenario runs do not start to clearly diverge until before ~ 2040 . Indeed, and examining the anomalies maps for SST (mean 2031 - 2034 minus mean 2015 - 2020, Fig. 6), it is clear that maximum surface warming is simulated with MPI under rcp4.5 (mean $\Delta\text{SST} \sim +0.4^\circ\text{C}$) while very little warming is simulated for MPI rcp8.5 (mean $\Delta\text{SST} \sim -0.003^\circ\text{C}$, Fig. 5C). In the two Ec-Earth forced runs the mean SST anomaly is very similar at around $+0.2^\circ\text{C}$ (Figs. 5B and 5D).

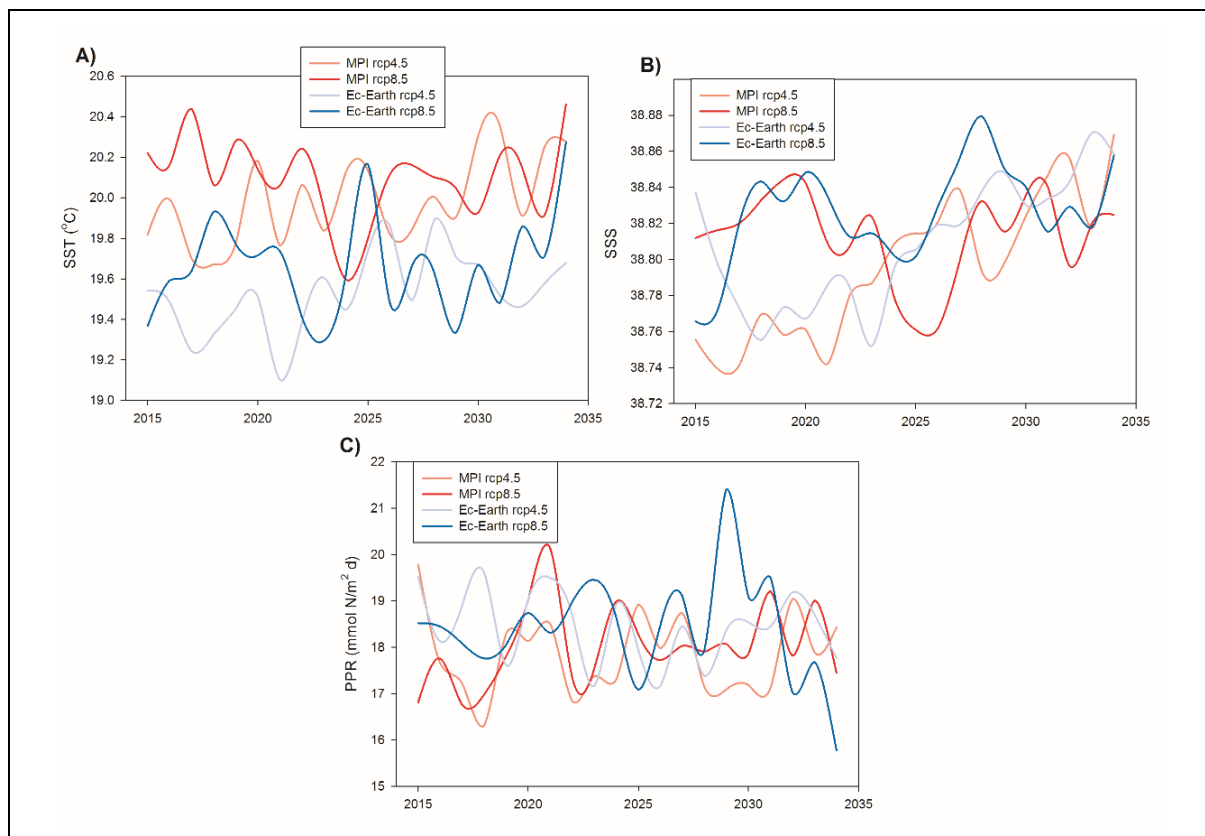


Figure 5. Time series of annual integrated SST, SSS and PPR for the four baseline runs (i.e., without modifications of the rivers conditions)

Almost the same could be said for the annual mean SSS values for all model runs (Fig. 5B) as interannual variability seems to be larger than any trend. In this case, however, it seems that after 2025 all model realizations tend to evolve towards higher salinity values. This is somehow confirmed by the anomaly maps for SSS (Fig. 7) where in all cases a mean positive value (difference between 2031 - 2034 and 2015 - 2018) is found, except for MPI under rcp8.5 where the difference is negative but very small (~ -0.0001).

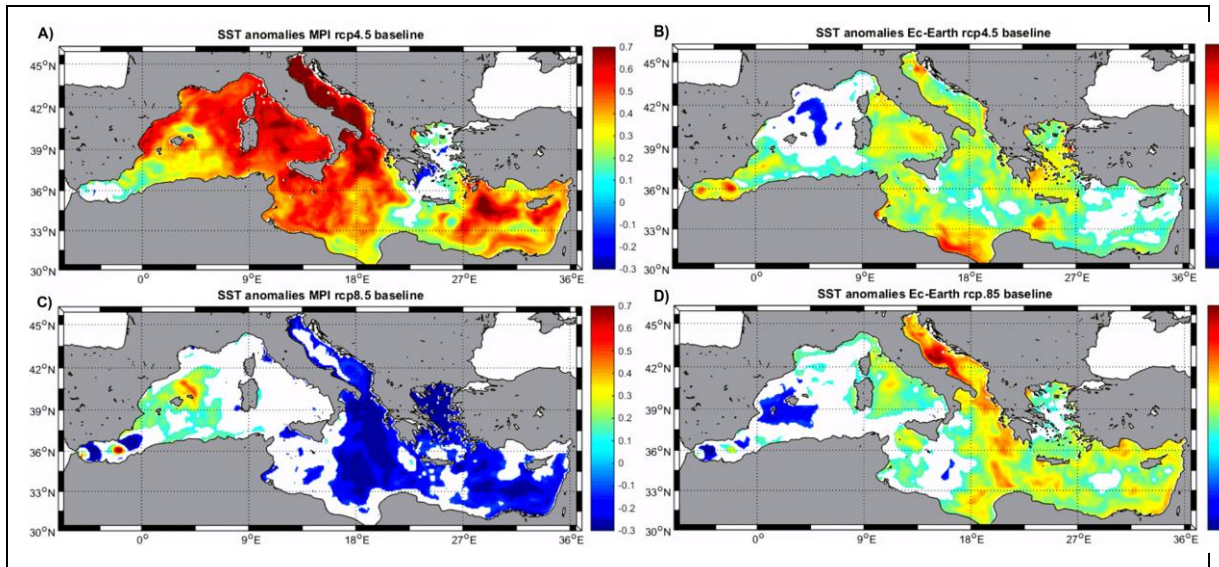


Figure 6. SST anomalies (2031 – 2034 vs. 2015 – 2018) for the four different baseline runs.

In general this warming and salinification trends correspond quite well with previous longer-term transient simulations for this basin (up to 2100, see Macias et al., 2015). A warmer atmosphere and an increase in evaporation are the main reasons for these trends. The lack of clear patterns and, particularly, of differences between the emission scenarios derive from the fact that rcp pathways are only substantially different after around 2040 – 2045 (IPCC, 2013).

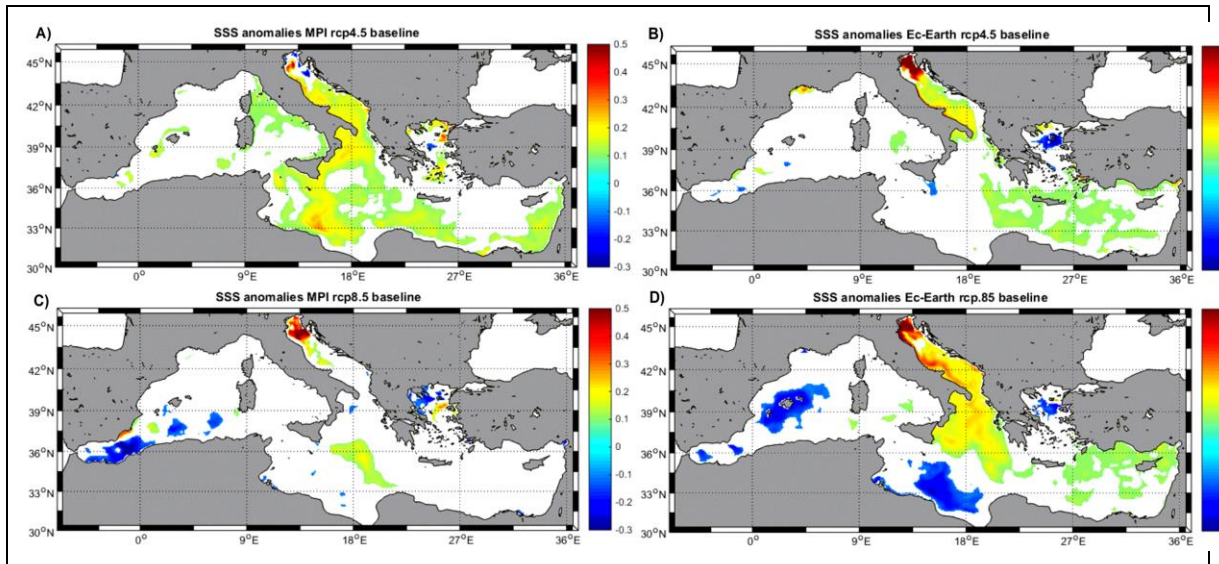


Figure 7. SSS anomalies (2031 – 2034 vs. 2015 – 2018) for the four different baseline runs.

For integrated PPR (Fig. 5C), again most of the variability of the time-series are located at the annual levels with no apparent trend in any of the scenarios. This is also in agreement with the results of Macias et al. (2015) using a very similar model configuration and river

conditions. In the anomaly maps for PPR (Fig. 8) it could be observed a marked regionalization, with some regions showing strongly positive anomalies (e.g., the central-eastern basin for MPI rcp8.5, Fig. 8C) and other regions becoming much more oligotrophic (e.g., the same region for Ec-Earth rcp8.5, Fig. 8D). Mean PPR anomalies are, however, typically small moving in between 2 and 7% of the mean annual PPR value.

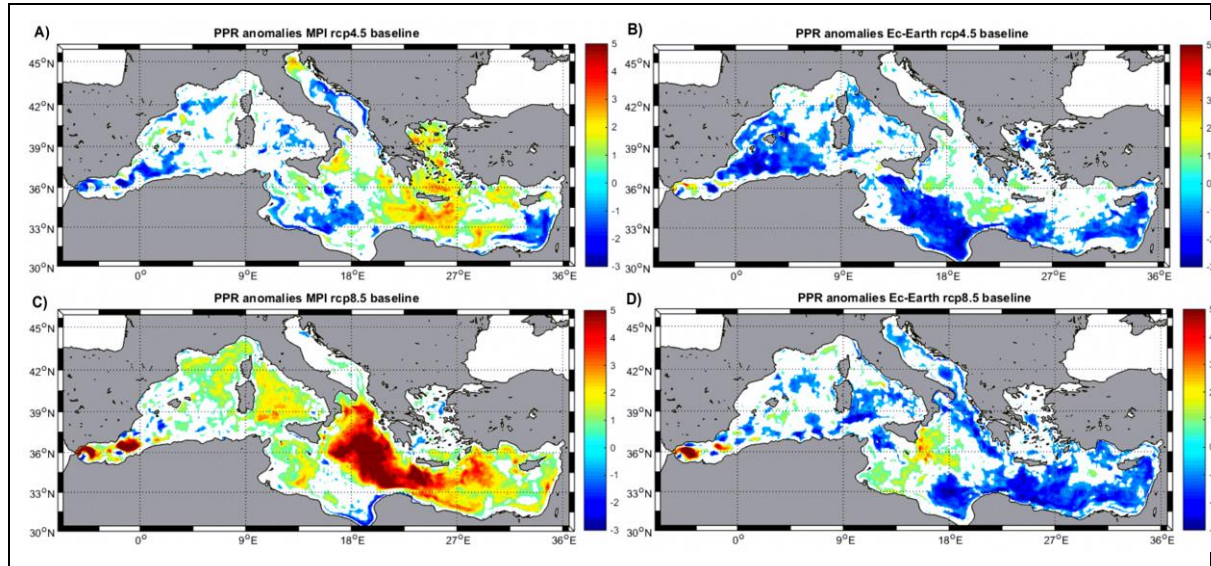


Figure 8. PPR anomalies (2031 – 2034 vs. 2015 – 2018) for the four different baseline runs.

In the longer (~100 years) model run performed in Macias et al. (2015) a relationship between surface density anomalies and PPR anomalies was found. In that case, regions where surface density increased showed higher biological productivity. The authors explained this pattern in relation with the vertical stability of the water column and, hence, the intensity of mixing and surface fertilization. For the present model runs, unfortunately, no clear relationship between surface density and PPR changes could be found, most likely because of the transient state of the system and the relatively short time-span that prevents clear relationships to emerge in the analysis. However, and considering that the simulations here were performed with the same modelling setup as the one in Macias et al. (2015), we can reasonably assume that the same processes are at play in the present case.

3.2 Evolution of the hydrodynamic and biogeochemical conditions in the rivers' scenarios runs

Effects on SST and SSS are identical for the two nutrients scenarios (see Figs. 9 and 10), only PPR values are different when the nutrient concentration in the rivers' waters are altered (Fig. 11). SST and SSS are going to be mainly affected by changes in freshwater flow which are identical in the two nutrient scenarios as explained before, this being the reason of the identical patterns shown in Figs. 9 and 10 for TG and GO.

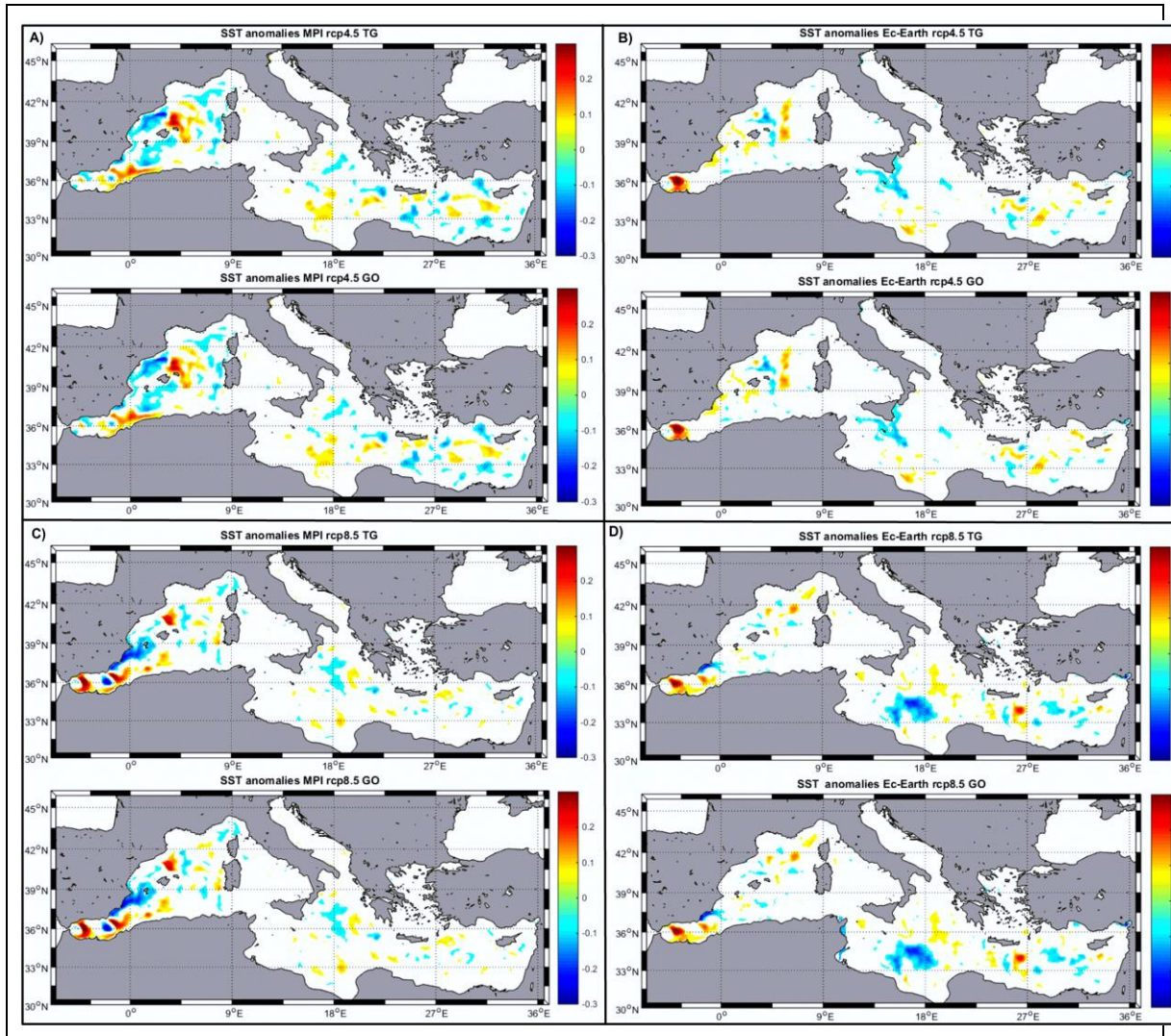


Figure 9. SST anomalies (2031 - 2034) for the four different runs. River scenario vs baseline

SST values change all-over the entire Mediterranean basin when freshwater flow is altered (Fig. 9) as also reported by Macias et al. (*submitted*). This widespread pattern is attributed to the alteration of the barotropic balance between the different water masses and seems to be confirmed by the detailed analysis on the vertical water stability properties performed in this previous work.

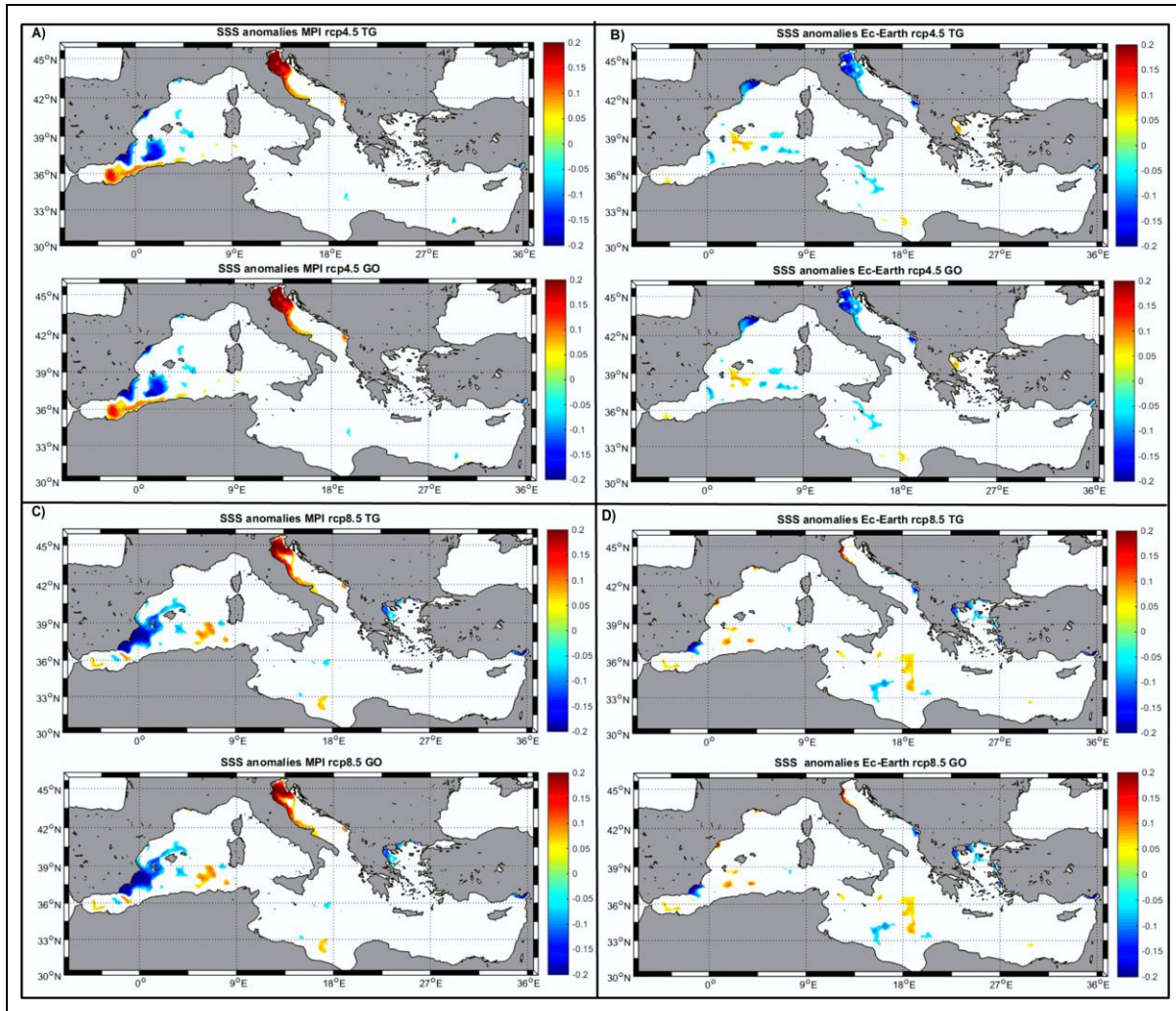


Figure 10. SSS anomalies (2031 - 2034) for the four different runs. River scenario vs baseline

SSS values, on the contrary, show a more regionalized pattern (Fig. 10) with the larger changes (both positive and negative) generally found in the vicinity of main rivers. The sign of the anomaly depends on the precipitation changes simulated by each GCM/rcp combination. For example for both MPI realizations (Figs. 10A and 10C) the Adriatic Sea and the Gulf of Lion become more saline, in line with the precipitation reduction simulated by these models realisations for the 'France' and 'Alpine' regions (Figs. 4A and 4C). On the contrary, for the Ec-Earth rcp4.5 simulations the Gulf of Lion and the northern Adriatic are simulated to become fresher (Fig. 10B) conditioned by the P increase in the central-north Mediterranean (Figs. 4B). For Ec-Earth rcp8.5 on the contrary, freshening is only evident in the southern Adriatic (Fig. 10D) linked with the precipitation increase in the 'Adriatic' river basin (Fig. 4D). Independently of the particular patterns for each model realization, the main conclusion with regard SSS is that more localized effects (compared with SST) could be observed when freshwater flow is altered.

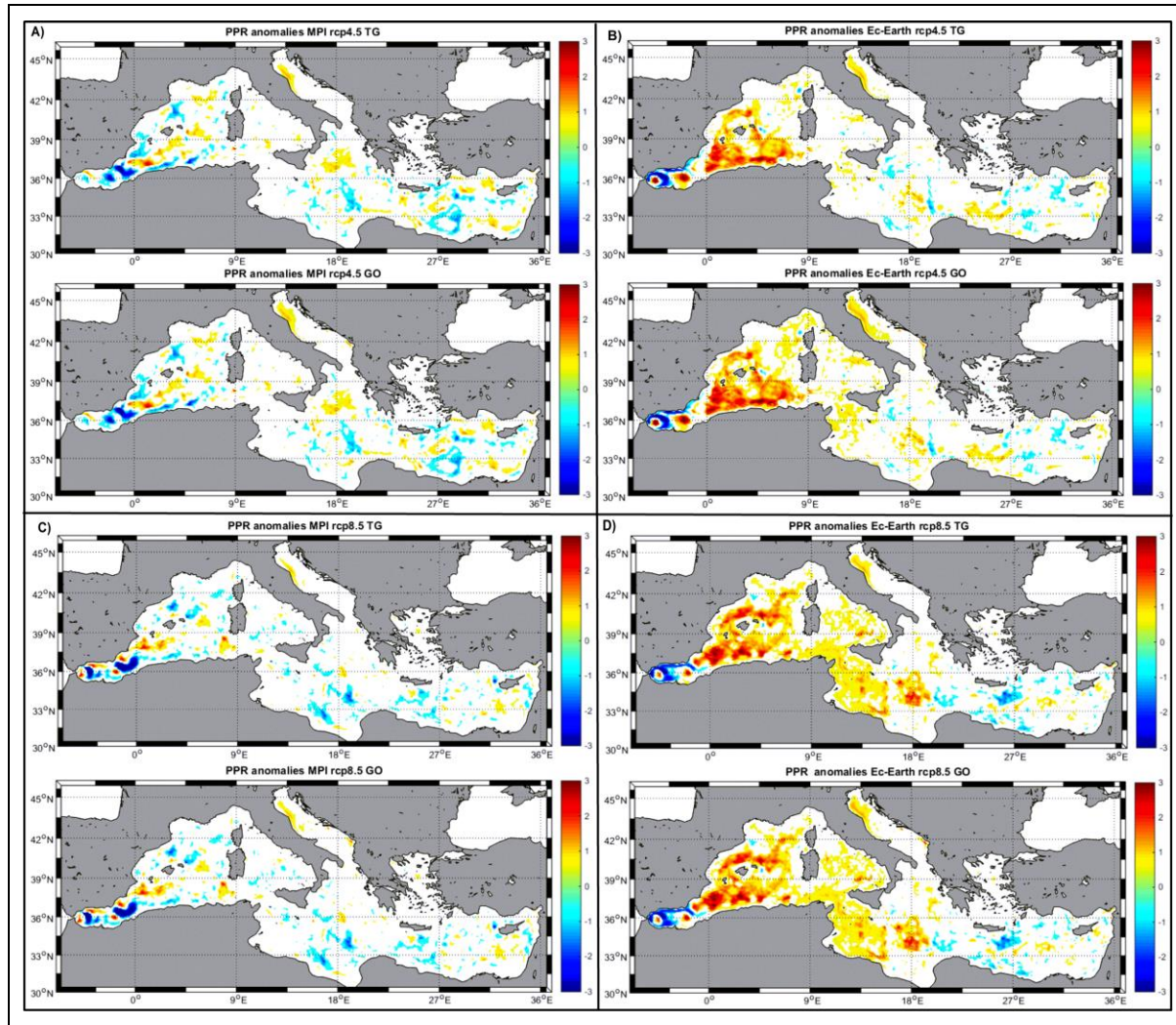


Figure 11. PPR anomalies (2031 - 2034) for the four different runs. River scenario vs baseline

For primary production levels, there are some differences between the two nutrients scenarios (as could be expected). For all GCMs/rcp combination the PPR mean value is higher in the GO nutrient scenario than in the TG although the total mean anomaly is quite low (around 0.05% in all cases, note the similarity of the PPR anomalies maps in Fig. 11). Another (better) way of looking at the differences in biological production induced by the nutrients scenarios is to map the surface chlorophyll (i.e., phytoplankton biomass) anomalies between the TG and GO cases as shown in Fig. 12. For all GCM/rcp combination there are increases of chlorophyll in the GO scenario in the Adriatic Sea and in the inner part of the Gulf of Lion, corresponding to an increase of the nutrient loads with respect to the TG scenario. In this case also the mean chlorophyll anomaly for all cases is quite low ($\sim 0.25\%$) although it is clear that for certain regions in the vicinity of main rivers' mouths the difference could reach $>14\%$.

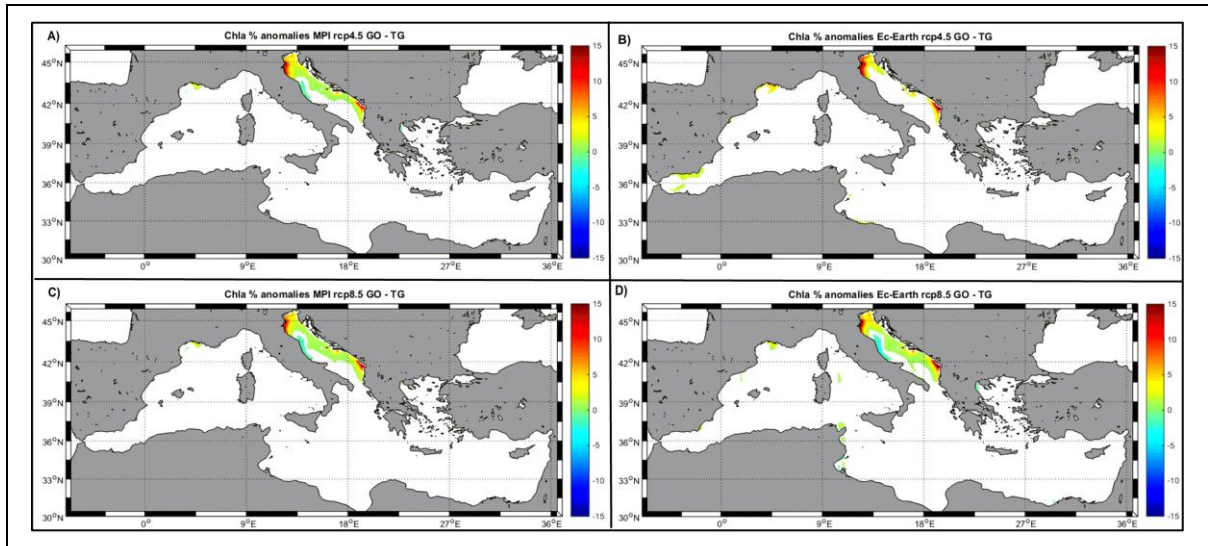


Figure 12. Chla anomalies (in %) for the four different runs. Worst case scenario (GO) vs best case scenario (TG)

As a final analysis, Chla seasonal anomalies have been computed for all scenarios runs. Typically (results not shown) bigger differences are found during the winter (December, January and February) months and smaller during late spring (April, May). This fact is reflected in the maps shown in Figure 13, where typically larger differences are visible during winter months. However, it is worth mentioning that the spatial pattern of the differences are very similar in the two seasons, coinciding also with the general anomalies maps in Fig. 12.

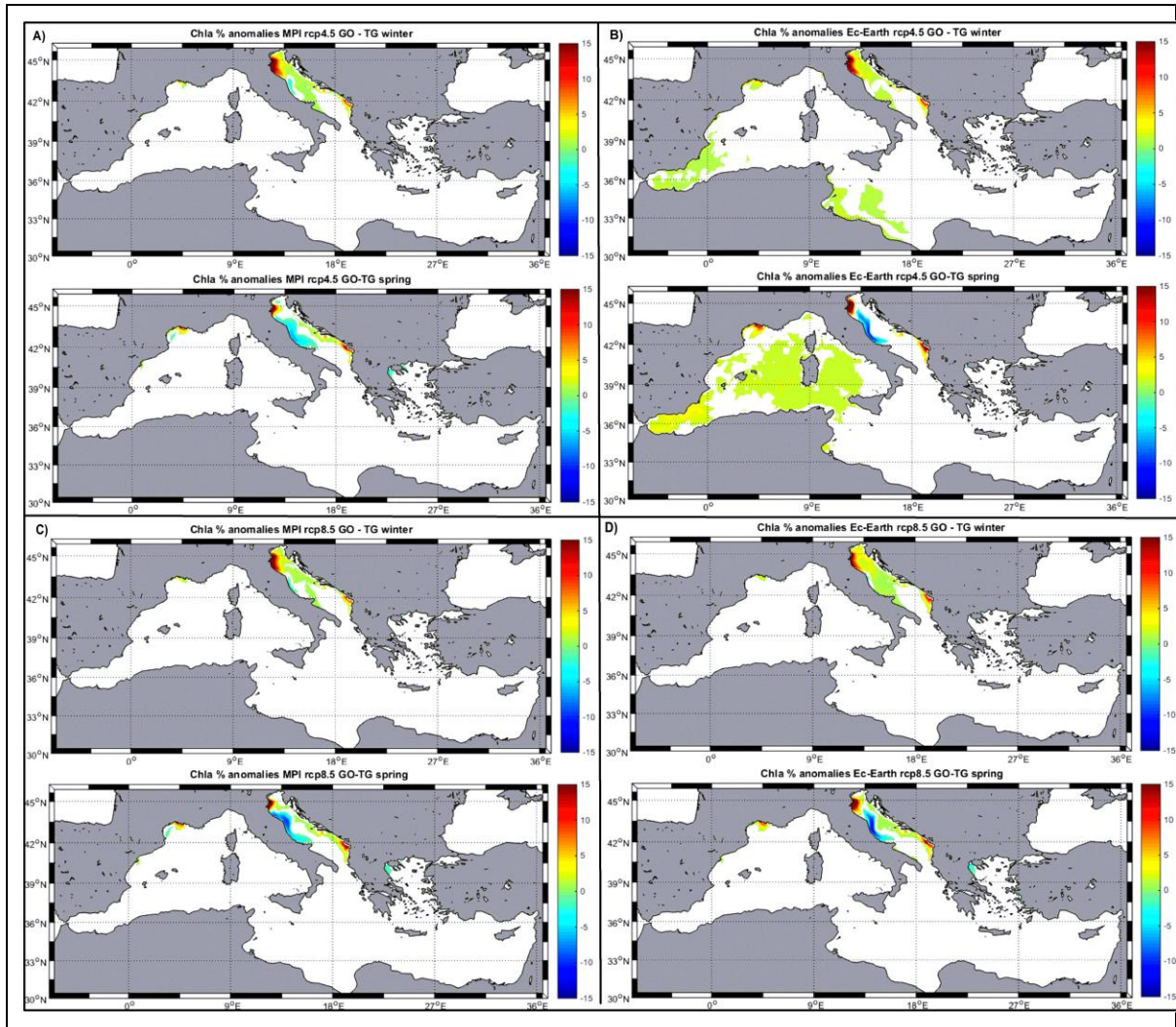


Figure 13. Chla anomalies (in %) for the four different runs. Worst case scenario (GO) vs best case scenario (TG) in winter (D,J,F) and spring (A,M).

4 Conclusion

The temporal evolution of mean annual basin properties (Fig. 5) clearly shows some of the limitation of the current generation climate models to produce consistent and reliable hydro-meteorological predictions in a medium-term horizon. As indicated by the time-series of mean surface properties, the total change in ~20 years is typically lower than the interannual variability and it is highly dependent of the model/rcp combination used. One of the reasons for this behaviour could be the lack of consistent, synchronous multidecadal variability in most GCMs while in the real climatic system such long-term oscillations are driving a substantial amount of the total variability (e.g., Macias et al., 2014c). Independent of the reasons, this exercise shows how cautious we must be when using climate model projections to create forecast scenarios in the near-medium future. It is, for example, possible that in this time-frame the mean annual SST in the Mediterranean decreases with respect to its actual value (see for example Fig. 6C) while still the general overall trend is a continuous background warming as exemplified in Macias et al. (2013a).

Regarding the lateral forcing excerpted by the freshwater inflow to the basin, different variables are affected diversely. For example, sea surface salinity shows anomalies regionally coherent and concentrated in the vicinity of main rivers' mouths. Adriatic and Aegean Seas are the more affected areas (Fig. 7) with the sign of the anomalies dependent on the precipitation changes simulated by the climate model (e.g., Fig. 4). Here it is also worth mentioning that in the east and south rivers' catchment areas the RCMs typically simulate large relative changes in P but no big impacts are observed in SSS. This could be related with the already low values of precipitation in these regions, a large percentual change of a small quantity is a rather small absolute change of freshwater flow.

On the other hand, sea surface temperature anomalies (Fig. 9) change throughout the entire basin and not only near the rivers' mouths. This fact has been explained by Macias et al. (*submitted*) as related with a change in the vertical stability of the water column induced by temperature variations. A small change in the overall properties of the Mediterranean Sea water masses could have a disproportionately large effect on vertical stratification and, hence, mixing. This same process could help explain the wide-spread scattered response of biological production anomalies (Fig. 10) as more mixing (colder waters) induced fertilization of the surface layer and enhances productivity.

Finally, the comparison of the two nutrients levels scenarios (TG and GO) for each individual RCM forcing (Fig. 12) allows to understand to what extend fertilization levels from riverine waters could affect the marine ecosystem of the Mediterranean Sea. In this two particular scenarios based on the '*Millenium assessment*' the variations for nitrate and phosphate are quite different (table 5). For nitrate, both scenarios predict a decrease that goes from -23% in TG to -2.6% in GO. Phosphate levels, on the other hand, increase in both scenarios: +13% in TG and +15% in GO. As phosphate is the main limiting nutrient in the Mediterranean (e.g., Siokou-Frangou et al., 2010) it is not surprising to find a relative low mean difference in phytoplankton biomass simulated for the two scenarios (mean ~ 0.25%). With another combination of nutrient levels reduction, bigger differences in phytoplankton production and biomass are to be expected.

In any case, it is also clear from Fig. 12 that the effects of changing nutrients in terms of phytoplankton biomass are not very widespread affecting between 3% and 5% of the total basin. It could also be noted that the spatial patterns of the anomalies are independent on the season and of the total mean change (see Fig. 13). It is, however, unclear whether a different set of nutrient scenarios including larger changes in phosphate concentrations could induce differences in a bigger fraction of the total basin.

In any case, the purpose of this report was to explore the potentialities of the MF to perform such scenario evaluations and not to assess the consequences of possible future changes in nutrient levels. It has been demonstrated that the system reacts logically to

the changes in the external forcings (both climatic, on freshwater flow and quality) being, thus, potentially usable for such exercises. This work has also served to understand how to construct future freshwater flow scenarios consistent with the climate changes reproduced by the atmospheric models. It has been shown that model performance and achieved results are strongly influenced by the reliability of the applied hydro-meteorological forcings. Regarding socio-economic scenarios affecting riverine water qualities, this preliminary work already indicate the larger importance (for the Mediterranean Sea ecosystems) of measures regulating phosphorous levels than those regarding nitrate. This could be of importance for river catchment management as sources of nitrate (e.g., agriculture and manure) are very different from those of phosphate (e.g., detergents and waste water treatments). Further work with the MF could help evaluate the necessary relative importance (always considering the effects on the marine ecosystem) of different management options in EU freshwaters.

References

- Bruggeman, J. and K. Bolding (2014), A general framework for aquatic biogeochemical models, *Environ. Modell. Software*, 61, 249-265.
- Burchard, H., and K. Bolding (2002), GETM, a general estuarine transport model. Scientific documentation, Technical report. Ispra, Italy, European Commission.
- Burchard, H., K. Bolding, W. Kuhn, A. Meister, T. Neumann and L. Umlauf (2006), Description of a flexible and extendable physical-biogeochemical model system for the water column, *J. Mar. Sys.*, 61, 180-211.
- Carpenter, S. R., P. L. Pingali, E. M. Bennett, and M. B. Zurek (Eds.) (2006), *Ecosystems and Human Well - Being, vol. 2, Scenarios*, 515 pp., Island Press, Washington, D. C.
- Dosio, A. and P. Paruolo (2011), Bias correction of the ENSEMBLES high-resolution climate change projections for use by impact models: Evaluation on the present climate, *J. Geophys. Res.*, 116, D161106.
- Dosio, A., P. Paruolo and R. Rojas (2012), Bias correction of the ENSEMBLES high resolution climate change projections for use by impact models: Analysis of the climate change signal, *J. Geophys. Res.*, 117, D171110.
- Dosio, A. (2016), Projections of climate change indices of temperature and precipitation from an ensemble of bias-adjusted high-resolution EURO-CORDEX regional climate models, *J. Geophys. Res. Atmos.*, 121, 5488–5511, doi:10.1002/2015JD024411.
- Garcia Gorriz E, Macias Moy D, Stips A, Miladinova-Marinova S. JRC Marine Modelling Framework in support of the Marine Strategy Framework Directive: Inventory of models, basin configurations and datasets . EUR 27885. Luxembourg (Luxembourg): Publications Office of the European Union; 2016. JRC100843
- Giorgi, F (2006), Climate change hot-spots. *Geophys. Res. Lett.*, 33, L08707.
- IPCC (2013). *Climate Change 2013: the Physical Science Basis. Contribution of working group I to the fifth assesment report of the intergovernmental panel on climate change*, Cambridge University Press.
- Ludwig, W., E. Dumont, M., Meybeck and S. Heussner (2009), River discharges of water and nutrients to the Mediterranean and Black Sea: Major drivers for ecosystem changes during past and future decades? *Prog. Oceanog.*, 80, 199-217
- Ludwig, W., Bouwman, A.F., Dumont, E. and Lespinas, F. (2010), Water and nutrient fluxes from major Mediterranean and Black Sea rivers: Past and future trends and their implications for the basin-scale budgets. *Global Biochemical Cycles*, 24, GB0A13.
- Macías, D., E. García-Gorríz and A. Stips (2013), Understanding the Causes of Recent Warming of Mediterranean Waters. How Much Could Be Attributed to Climate Change? *Plos One*, 8(11), e81591.
- Macías, D., E. García-Gorríz, C. Piroddi and A. Stips (2014a), Biogeochemical control of marine productivity in the Mediterranean Sea during the last 50 years. *Glob. Biochem. Cycles*, 28, 897-907.
- Macías, D., A. Stips and E. Garcia-Gorriz (2014b), The relevance of deep chlorophyll maximum in the open Mediterranean Sea evaluated through 3D hydrodynamic-biogeochemical coupled simulations. *Ecol. Model.*, 281, 26-37.
- Macias D., A. Stips, E. Garcia-Gorriz (2014c), Application of the Singular Spectrum Analysis Technique to Study the Recent Hiatus on the Global Surface Temperature Record. *PLoS ONE* 9(9): e107222. doi:10.1371/journal.pone.0107222
- Macias, D., E. Garcia-Gorriz and A. Stips (2015), Productivity changes in the Mediterranean Sea for the twenty-first century in response to changes in the regional atmospheric forcing, *Front. Mar. Sci.*, 2(79).

- Macías, D., E. Garcia-Gorriz and A. Stips, A (2016a), The seasonal cycle of the Atlantic Jet dynamics in the Alboran Sea: direct atmospheric forcing versus Mediterranean thermohaline circulation, *Ocean Dyn.*, 66, 137-151.
- Macías, D., E. Garcia-Gorriz, A. Stips, A. Dosio and K. Keuler (2016b), Obtaining the correct sea surface temperature: bias correction of regional climate model data for the Mediterranean Sea. *Clim. Dyn.*, in press, doi: 10.1007/s00382-016-3049-z
- Macías, D., E. Garcia-Gorriz, A. Stips, A. (*submitted*), Hydrological and biogeochemical response of the Mediterranean Sea to freshwater flow changes for the end of the 21st century. *J. Mar. Sys.*
- Meinshausen, M., S.J. Smith, K. Calvin, J.S. Daniel, M.L.T. Kainuma, J.F. Lamarque, K. Matsumoto, S.A. Montzka, S.C.B. Raper, K. Riahi, A. Thomson, G.J.M. Velders and D.P.P. van Vuuren (2011), The RCP greenhouse gas concentrations and their extensions from 1765 to 2300, *Climat. Chang.*, 109(1-2), 213-241.
- Najjar, R. G., H.A. Walker, P.J. Anderson, E.J. Barron et al. (2000), The potential impacts of climate change on the Mid-Atlantic coastal region, *Clim. Res.*, 14, 219-233.
- Neumann, T (2000), Towards a 3d-ecosystem model of the Baltic Sea. *J. Mar. Sys.*, 25, 405-419.
- Siokou-Frangou, I., Christaki, U., Mazzocchi, M.G., Montresor, M., Ribera d'Alcalá, M., Vaqué, D., Zingone, A. (2010), Plankton in the open Mediterranean Sea: a review. *Biogeosciences* 7: 1543-1586.
- Somot, S., F. Sevault, M. Déqué (2006), Transient climate change scenario simulation of the Mediterranean Sea for the twenty-first century using a high-resolution ocean circulation model, *Clim. Dyn.*, 27(7-8), 851-879.
- Stips, A., K. Bolding, T. Pohlman and H. Burchard (2004), Simulating the temporal and spatial dynamics of the North Sea using the new model GETM (general estuarine transport model), *Ocean Dyn.*, 54, 266-283.
- Stips A, Dowell M, Somma F, Coughlan C, Piroddi C, Bouraoui F, Macias Moy D, Garcia Gorriz E, Cardoso A, Bidoglio G, authors. Towards an integrated water modelling toolbox. European Commission; 2015. JRC92843

List of abbreviations and definitions

AM: 'Adaptative Mosaic' socio-economic scenario
DG: Directorate General of the European Commission
EU: Europe/European
GETM: General Estuarine Transport Model
GCM: Global Climate Model
GO: 'Global Orchestration' socio-economic scenario
IPCC: Intergovernmental Panel for Climate Change
JRC: Joint Research Centre
MEDAR: Mediterranean Data Archeology and Rescue database
MedERGOM: Mediterranean version of the ERGOM biogeochemical model
MF: Modelling Framework
OS: 'Order from Strength' socio-economic scenario
PPR: primary production rate
RCM: Regional Circulation Model
rcp: green-house gasses emission scenario
SSS: Sea surface salinity
SST: Sea surface temperature
TG: 'Technogarden' socio-economic scenario
WISE: Water information system for Europe

List of figures

Figure 1. Modelling Framework (MF) scheme as used in the present report.

Figure 2. Model domain, bathymetry (background scale), included rivers (red stars) and polygons (yellow lines) defining the different regions considered for rivers' basins.

Figure 3. Relative change on P for each catchment area for MPI RCP4.5 scenario (A), EC-Earth RCP4.5 scenario (B), MPI RCP8.5 scenario (C) and EC-Earth RCP8.5 scenario (D). The 0% change level is indicated with a black line and the mean monthly change with a bold grey line.

Figure 4. Mean P change (%) for each river basin district and model/RCP combination.

Figure 5. Time series of annual integrated SST, SSS and PPR for the four baseline runs (i.e., without modifications of the rivers conditions).

Figure 6. SST anomalies (2031 – 2034 vs. 2015 – 2018) for the four different baseline runs.

Figure 7. SSS anomalies (2031 – 2034 vs. 2015 – 2018) for the four different baseline runs.

Figure 8. PPR anomalies (2031 – 2034 vs. 2015 – 2018) for the four different baseline runs.

Figure 9. SST anomalies (2031 – 2034) for the four different runs. River scenario vs baseline

Figure 10. SSS anomalies (2031 – 2034) for the four different runs. River scenario vs baseline.

Figure 11. PPR anomalies (2031 – 2034) for the four different runs. River scenario vs baseline.

Figure 12. Chla anomalies (in %) for the four different runs. Worst case scenario (GO) vs best case scenario (TG).

Figure 13. Chla anomalies (in %) for the four different runs. Worst case scenario (GO) vs best case scenario (TG) in winter (D,J,F) and spring (A,M).

List of tables

Table 1. Institutes/modelling groups providing the atmospheric model data used in the present contribution.

Table 2. Basin names and included rivers.

Table 3. Computed annual changes in freshwater flow for the different model/rcp combinations.

Table 4. Socio-economic scenarios considered in the Millennium Ecosystem Assessment.

Table 5. Relative change of nutrient concentration in freshwater for the different catchments and under the different scenarios.

Table 6. Description of the different model runs.

***Europe Direct is a service to help you find answers
to your questions about the European Union.***

Freephone number (*):

00 800 6 7 8 9 10 11

(*) The information given is free, as are most calls (though some operators, phone boxes or hotels may charge you).

More information on the European Union is available on the internet (<http://europa.eu>).

HOW TO OBTAIN EU PUBLICATIONS

Free publications:

- one copy:
via EU Bookshop (<http://bookshop.europa.eu>);
- more than one copy or posters/maps:
from the European Union's representations (http://ec.europa.eu/represent_en.htm);
from the delegations in non-EU countries (http://eeas.europa.eu/delegations/index_en.htm);
by contacting the Europe Direct service (http://europa.eu/eurodirect/index_en.htm) or
calling 00 800 6 7 8 9 10 11 (freephone number from anywhere in the EU) (*).

(*) The information given is free, as are most calls (though some operators, phone boxes or hotels may charge you).

Priced publications:

- via EU Bookshop (<http://bookshop.europa.eu>).

JRC Mission

As the science and knowledge service of the European Commission, the Joint Research Centre's mission is to support EU policies with independent evidence throughout the whole policy cycle.



EU Science Hub

ec.europa.eu/jrc



@EU_ScienceHub



EU Science Hub - Joint Research Centre



Joint Research Centre



EU Science Hub

